Development of a Crop Edge Line Detection Algorithm Using a Laser Scanner for an Autonomous Combine Harvester

Chan Woo Jeon[1], Hak-Jin Kim[1*], Xiong Zhe Han[1], Hee Chang Moon[2]

[1]Dept. of Biosystems Engineering and Biomaterials Science, College of Agriculture and Life Sciences, Seoul National University, Seoul, Korea

[2]Unmmand Solution Co., Ltd, Seoul, Korea

Abstract. The high cost of real-time kinematic (RTK) differential GPS units required for autonomous guidance of agricultural machinery has limited their use in practical auto-guided systems especially applicable to small-sized farming conditions. A laser range finder (LRF) scanner system with a pan-tilt unit (PTU) has the ability to create a 3D profile of objects with a high level of accuracy by scanning their surroundings in a fan shape based on the time-of-flight measurement principle. This paper describes the development of a LRF-based autonomous navigation algorithm for a head-feeding rice combine harvester that could automatically follow straight rice rows based on real-time detection of rice uncut edges. A motor-driven crawler type platform operated on a myRIO real-time controller was constructed to develop a steering control algorithm suitable for such a tracked type-driving mechanism. Noise data existing in raw dataset were removed to extract rice row profiles without unpredictable disturbances by using the revised random sample consensus (RANSAC) method. Boundary points between uncut and cut edges were then determined using the maximum method. The 3D points defined in terms of the LRF sensor coordinates were converted into the vehicle coordinates by considering the platform movement and PTU rotation in order to create a 3D field map of uncut edges for autonomous harvesting. A PID steering control algorithm based on a linear relationship between the lateral deviation and heading error of the mobile platform was implemented. Laboratory tests showed that the PTU operation improved the ability of the uncut edge detection algorithm to detect the target in the presence of interfering objects as compared to that measured without use of the PTU, showing a decrease in lateral RMSE from 21.8 to 5.7 cm whereas there was little change in heading RMSE < 2 deg. A fundamental navigation experiment showed that the mobile platform-mounted LRF scanner system could guide the motor-driven platform following straight and curved edge lines of artificial targets with an acceptable level of oscillation at a traveling velocity of 0.14 m/s. Therefore, the use of a laser based real-time path generation and tracking

algorithm would be feasible in automatically guiding the rice combine harvester.

Keywords. *Autonomous navigation algorithm, Laser scanner, Pan-tilt unit, Crop edge line detection, 3D crop profile, RANSAC, Tracked vehicle*

1. Introduction

Accurate steering of agricultural machinery within rowed crop fields to perform various farm operations, such as planting, spraying, and harvesting is a tedious task for drivers (Kise et al., 2005) Autonomous or semi-autonomous navigation systems can help to automatically guide the machinery or the drivers to easily steer the machines following crop rows to perform the required farm operations. In the last decades, many studies about automated guidance systems have been conducted using various sensors, including global positioning (GPS) systems (Iida et al., 2013; X. Z. Han et al., 2015), machine-vision systems (T. Torii et al., 2000; M. Kise et al., 2005) and laser range finders (A.Tofael et al., 2006; C. Barawid Jr et al., 2007). However, the results of the previous studies showed several limitations in being used in outdoor environments in terms of performance and reliability. For instance, the accuracy of an available GPS system was strongly dependent on its price and frequent compensation for the GPS signal offsets was required to obtain reliable data of the GPS system used. Since varying light conditions may cause machine-vision data to be distorted, the use of a camera is limited in outdoors. On the other hand, the use of a Laser Range Finder (LRF) sensor could be suitable for detecting landmarks in outdoor conditions with high accuracy within 50 mm measured at relatively long distances (<100 m) because such Laser rangefinder (LF) technology is not be affected by ambient lighting conditions. Thus, LF technology can be more reliable in an agricultural environment (T. Coen et al., 2008). Since the measurable distance and measurement accuracy of the LRF sensors are directly related to the price of the LRF sensor, Choi et al. (2014) used a pan-tilt unit (PTU) to automatically rotate the angle of a relatively low-cost LRF sensor and acquired a 3D profile of soybean crops instead of using conventional expensive LRF sensors. In addition, a fusion approach to use GPS and LRF sensors was conducted by Cho et al. (2015) to detect the crop height and edge points of rice based on the generation of a 3D field rice row. The results showed that the edge point detection method was affected by unpredictable disturbance and inevitable lateral deviation caused by ear of rice. An another detecting edge point method based on the LRF was proposed using the Otsu's threshold method along with the PTU and the lateral deviations of the prototype system relative to the reference targets were evaluated (Z. Teng at el.,2016).

The overall objective of this study was to develop a robust autonomous navigation algorithm based on a LRF sensor for accurately guiding a head-feeding combine harvester following the rice row. To accomplish this objective, a RANSAC filtering method and a detection algorithm of rice edge in conjunction with the use of a PTU were implemented. The feasibility of the developed algorithm for the noise removal and edge detection was investigated using artificial landmarks installed in the laboratory. A crawler type motor-driven platform operated on a myRIO real-time controller was constructed to develop a steering control algorithm because it is commonly used as the driving equipment of a head-feeding rice combine harvester.

---

2. Materials and Methods

2.1. System setup

A motor-driven tracked vehicle was constructed to evaluate the performance of autonomous navigation and control algorithms developed under the laboratory conditions. As shown in Fig. 1, two motors were installed in left and right crawlers, respectively, to independently control the rotational speeds of the two different tracked vehicles based on a closed loop system using rotary encoders. A NI myrio board (National Instruments, Texas, America) was used to integrate the low-level control of the tracked motion and communicate with a programmable computer mounted on a mobile platform via the control area network (CAN) bus. A LMS511-PRO 2D laser range finder (LRF) scanner (SICK, Waldkirch, Germany) was mounted on the top of the platform roof about 2.1 m above the ground. The LRF sensor used in the study showed a maximum detection range of 80 m and a scanning angle of 190 deg. The sampling rate and resolution setup were 50 Hz and 0.5 deg, respectively. To acquire three-dimensional field information, a pan-tilt unit (PTU) was developed using a SM23165DT smart motor (Moog Animatics, California , USA) and a PGX-H-62 decelerator (ATG, Seoul, Korea) to provide a tilt rotation by changing the tilting angles of up to $\pm$30 deg. A SBG-Ellipse-E IMU sensor (SBG Systems, Rueil-Malmaison, France) was installed in the PTU to collect information about the platform attitude and the tilting angle of the PTU at every cycle of measurement. Fig. 2 shows the components of the experimental navigation system constructed in the laboratory.
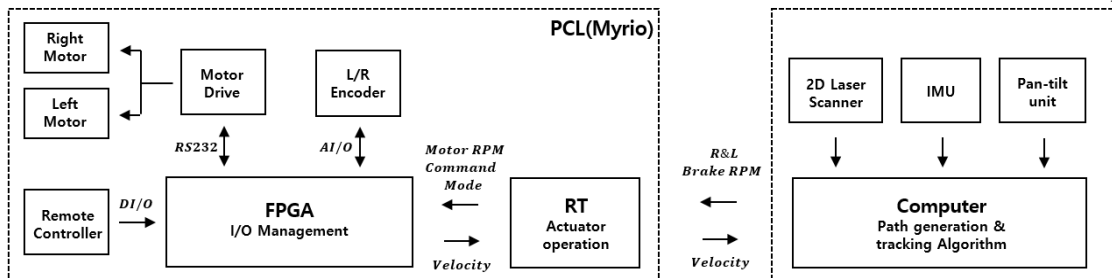

Fig 1. Block diagram of the system components
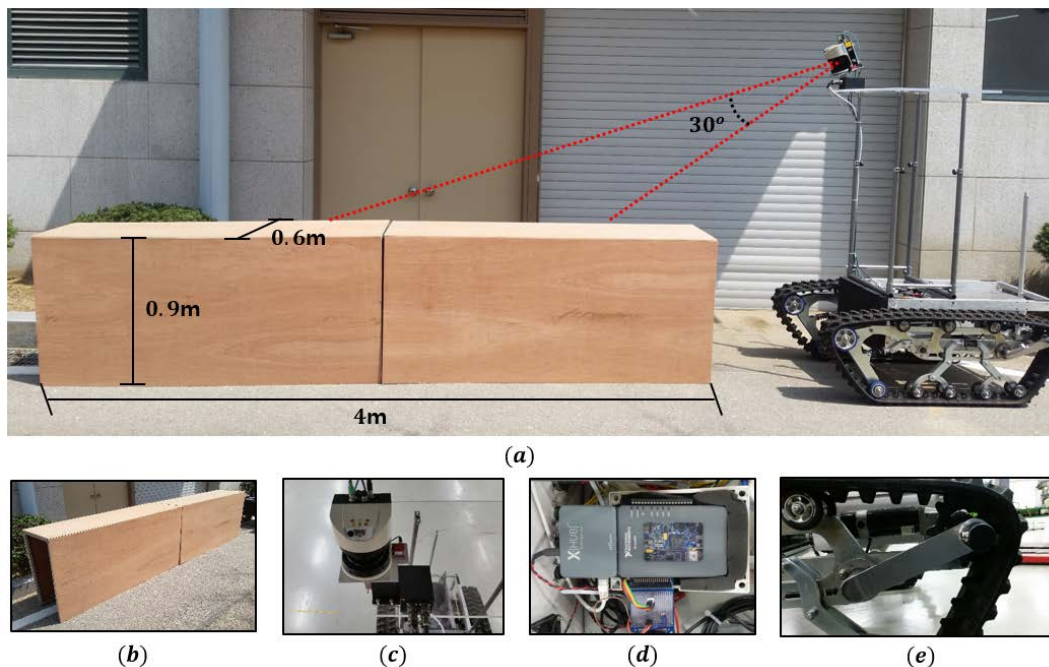

(a)

(b)   (c)   (d)   (e)

Fig 2. Experimental navigation system and its components (a) Tracked Vehicle; (b) Lab condition crop profile; (c) Laser scanner and IMU with pan-tilt unit; (d) programmable logic control board, Myrio; (e) Encoder

2.2. Real-time navigation control algorithm

As shown in Fig. 3, the real-time navigation control algorithm developed in the study was composed of four steps. Firstly, range data of all objects including landmarks and other noise were collected. A random sample consensus (RANSAC) algorithm was then applied to extract accurate 2D profiles of crop and ground data on every sampled distance data array. Secondly, an edge point was calculated using the maximum distance method that considers geometrical lateral deviations caused by an ear of crop. Thirdly, to construct 3D profiles of the uncut and cut crops and a tracking line for the vehicle platform, data categorized as the target objects were collected during one cycle of PTU. Because the PTU was continuously rotated and the vehicle was in motion, a compensation procedure for the position change was added. Finally, the tracking line was detected based on 2nd RANSAC filtering and operating parameters such as lateral deviations and heading errors were calculated. A steering control algorithm was then implemented to minimize the operating parameters as each of velocities was transferred to the my-RIO controller in order to navigate the tracked vehicle along the predefined line.
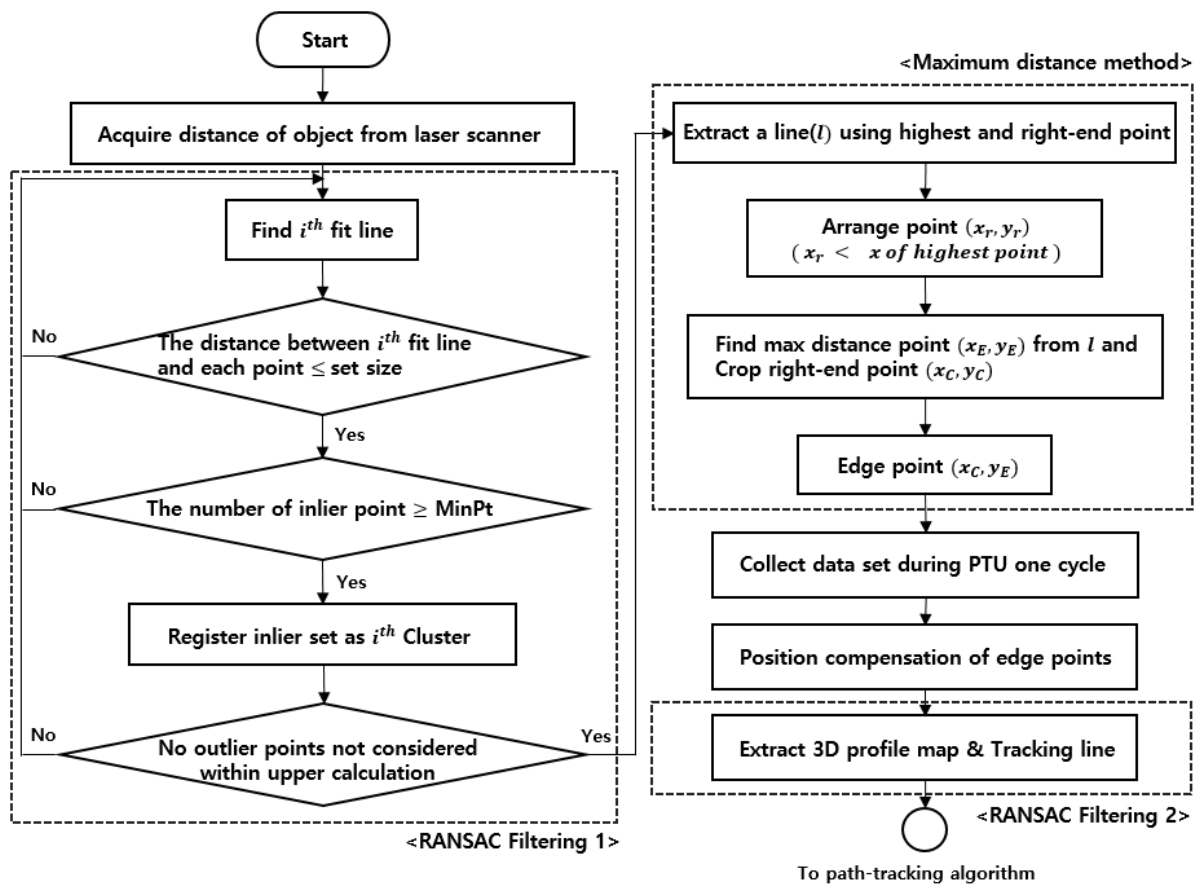

Fig 3. Flowchart of data processing for auto navigation system

2.2.1. Extraction of 3D crop profile with RANSAC algorithm

In designing a LRF-based navigation algorithm, it is important to extract 3D profiles of crops by choosing appropriate landmarks and optimal methods in order to determine reliable path lines. The LRF system could detect all distance data including noise signals, such as a stack of straws and other landmarks adversely affecting the target detection. To remove such unwanted signals, a RANSAC algorithm that can predict model parameters from a set of observed data containing outliers was applied to detect the uncut crop edge from the 3D profile map generated in real-time.

Since an original RANSAC algorithm estimates only one model from one specific dataset, as shown in Fig.4, in some cases, two bad results can be obtained. That is, because the algorithm is basically applied based on a certain probability, both crops and ground landmarks could be regarded as inlier points, thereby providing missing landmarks. As the other case, since the original RANSAC method considered a whole set of landmarks a single landmark, only one fitting line can be obtained. To overcome the problems, a modified RANSAC algorithm was implemented in the study following four main procedures described below:

1) Five points obtained with the Laser scanner are randomly selected and a fitting line is constructed by means of linear regression
2) Distances between remaining points and the fitted line are calculated and the corresponding points are defined as inlier or outlier points, respectively, depending on a threshold value which was 3 cm in this experiment
3) Additional examination is performed to see if the number of data selected as the inlier set is larger than the minimum number of points (MinPt). If the inlier set is determined as an appropriate landmark, it is registered as i^{th} cluster. In this experiment, the MinPt used was 20.
4) An upper process is repeated using the same dataset to detect all fitted lines by using remaining uncategorized points until all outlier points were used.
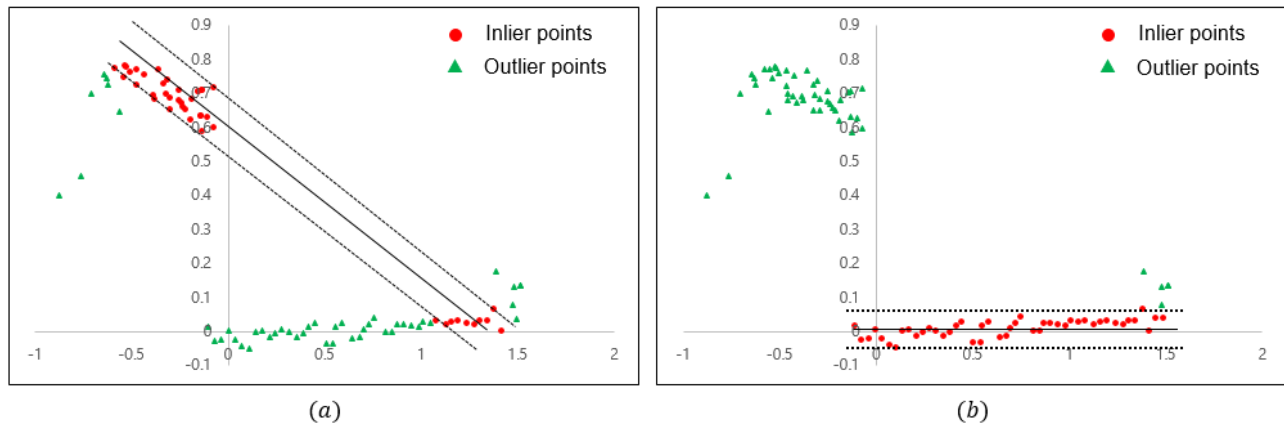

(a)　　　　　　　　　　　　　　　　(b)

Fig 4. Examples showing bad results obtained from the original RANSAC algorithm for (a) missing landmarks and (b) extracting only one landmark

2.2.2. Edge detection method

The method to detect the cut edges of the rice crop used in the study had three steps. Firstly, the data obtained with the LRF based on the polar coordinates, θ_{Laser} and ρ_{Laser}, were converted into the Cartesian coordinates using Eq.1. Secondly, the point (x_{max}, y_{max}) having a maximum value and the point (x_{end}, y_{end}) located on the extreme right were extracted. Assuming that combine harvesting operations are conducted in the direction of counter-clockwise, the uncut crop field was located in left-side as shown in Fig. 4. Lastly, the cut edge was determined using Eq.2 which identified a maximum distance from the foot of the perpendicular line (Kimberling, 1998).

$$\begin{bmatrix} x_{Laser} \\ y_{Laser} \\ z_{Laser} \end{bmatrix} = \begin{bmatrix} \rho_i \cos(\theta_i) \\ \rho_i \sin(\theta_i) \sin(\theta_{Laser}) \\ h_{Laser} - \rho_i \sin(\theta_i) \cos(\theta_{Laser}) \end{bmatrix}$$

(1)

where ρ_i is reflection distance and θ_i is measurement angle, θ_{laser} is tilt angle and h_{laser} is height of LRF.

$$d = \frac{|(y_e - y_m)(x - x_e) - (x_e - x_m)(y - y_e)|}{\sqrt{((x_m - x_e)^2 - (y_m - y_e)^2)}} \qquad (2)$$

where (x_{max}, y_{max}) is maximum height point and (x_{end}, y_{end}) is right end point

The straightness of the laser light can cause inevitable errors while producing geometrical offsets in detecting the edge points of 3D objects when the scanner is fixed at a point. Fig. 5 shows the schematics of geometrical limitation when the LRF without a pan-tilt unit collected cut edges. The accurate edge point is not detected due to such a 3D profile. A method to detect accurate edge points was designed to reduce the lateral deviation errors to properly navigate the mobile platform.
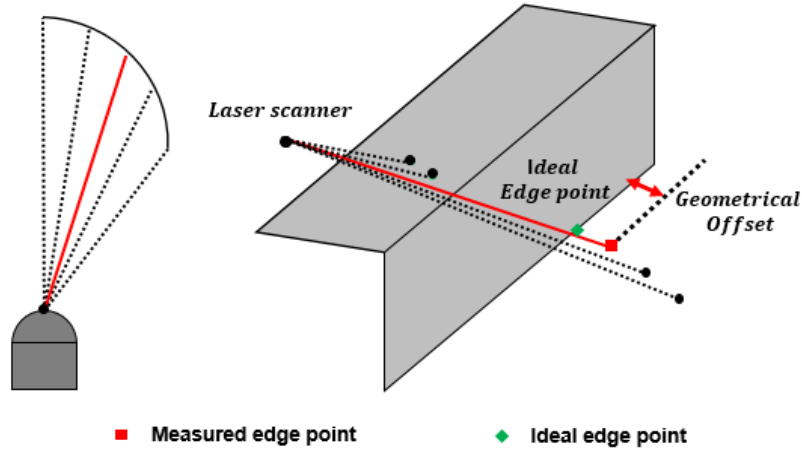

Fig 5. Geometrical limitation of laser scanner caused by characteristic of straightness

When the edge points were selected, index numbers from the right-end side to the left-end side were assigned to each LRF data. As shown in Fig. 6, uncut crop edge points were changed by moving uncut crop points to the right direction and moving cut crop points to the left direction (Eq. 3).

$$\begin{bmatrix} x_{new\ Edge} \\ y_{new\ Edge} \\ z_{new\ Edge} \end{bmatrix} = \begin{bmatrix} x_{Crop\ end,i+1} \\ y_{Crop\ end,i+1} \\ z_{Edge,i} \end{bmatrix} \qquad (3)$$

where $x_{Edge,i}$, $x_{Edge,i}$, $z_{Edge,i}$ are extracted using the edge detection method, $x_{Crop\ end,i+1}$, $y_{Crop\ end,i+1}$, $z_{Crop\ end,i+1}$ were crop right-end point, i and i+1 were index number.
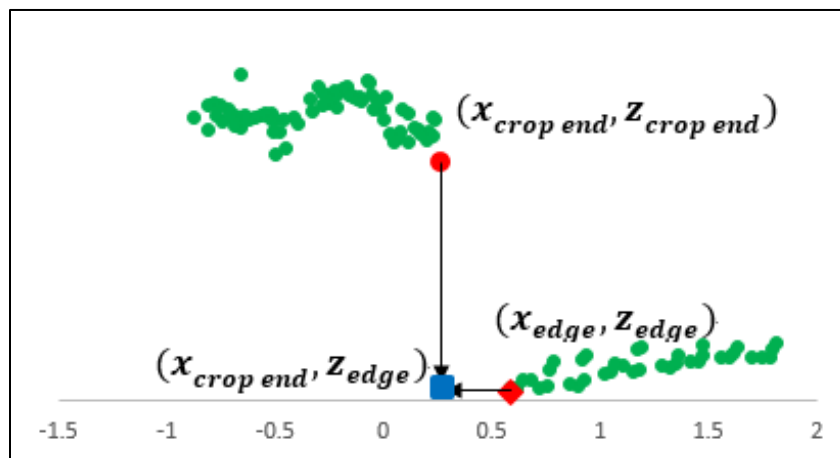

Fig 6. The definition of revision edge point

The uncut crop edge points were converted into data in the Cartesian coordinates system by considering the rotation of the PTU and the movement of the tracked vehicle using Eqs. (4) and (5).

$$\begin{bmatrix} x_{Laser} \\ y_{Laser} \\ z_{Laser} \end{bmatrix} = \begin{bmatrix} \rho_i \cos(\theta_i) + x_{tracked\ vehicle,k} \\ \rho_i \sin(\theta_i) \sin(\theta_{Laser}) - L_{bar} \sin(\theta_{Laser}) + y_{tracked\ vehicle,k} \\ h_{Laser} - \rho_i \sin(\theta_i) \cos(\theta_{Laser}) + L_{bar}(1 - \cos(\theta_{Laser})) \end{bmatrix} \tag{4}$$

$$\begin{bmatrix} x_{tracked\ vehicle,k+1} \\ y_{tracked\ vehicle,k+1} \end{bmatrix} = \begin{bmatrix} x_{tracked\ vehicle,k} + v_{c,k}\ \Delta t\ \sin(\theta_{yaw}) \\ x_{tracked\ vehicle,k} + v_{c,k}\ \Delta t\ \cos(\theta_{yaw}) \end{bmatrix} \tag{5}$$

$$v_{c,k} = \frac{v_{r,k} + v_{l,k},}{2} \tag{6}$$

where L_{bar} is PTU bar length, $v_{c,k}$ is the forward velocity of vehicle, Δt is sampling time, θ_{yaw} is yaw angle measured by IMU and $v_{r,k}, v_{l,k}$ are right end left crawler velocity respectively

2.2.4. The Navigation control

Fig. 7 shows the schematic diagram of the navigation control system. When the edge line was detected, the lateral deviation and heading error were calculated. The lateral deviation was defined as a difference between the right-end of cutter of the tracked vehicle and the reference tracking line. Heading error was defined as a relative angle between the reference heading angle estimated based on the edge detection method line and the yaw angle of the vehicle. The navigation variable of the tracked vehicle was determined from the lateral deviation and heading error using Eq. 7, which was then applied to a PID process variable to be minimized adaptively.

$$\delta\ (\text{Navigation variable}) = \alpha \times \Delta L + \beta \times \Delta\theta \tag{7}$$

where α is lateral deviation coefficient, β is heading error coefficient, ΔL(m) is Lateral deviation and $\Delta\theta$(°)is heading error

Coefficients of a PID-based steering controller and a navigation system were determined by trial-and-error method, i.e., Kp, Ki, and Kd values were 4, 0.1, and 0.01, respectively, and all of α and β values were 0.5. Steering of the vehicle platform was performed by independently changing the velocities of left and right crawlers.
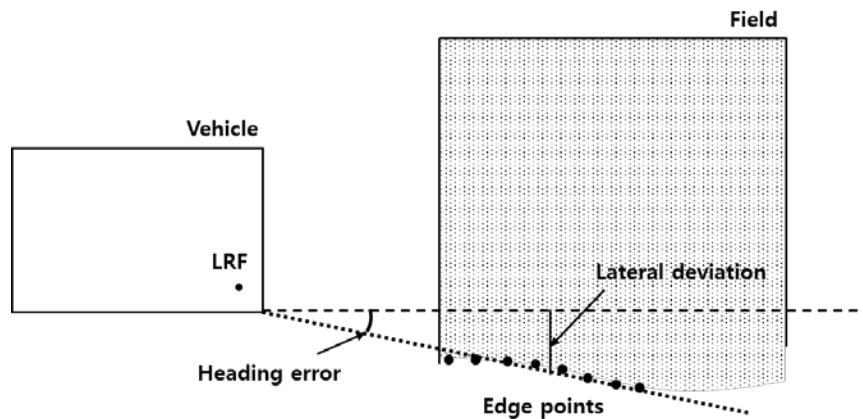

Fig 7. The schematic diagram of an auto-guidance control

2.3. Laboratory tests

The experiment was conducted in lab condition to evaluate the performance of the proposed edge detection algorithm. As shown in Fig. 2 (b), small sized, i.e., 0.6 x 4 x 0.9 m^3 (width x length x height), artificial crop profile made of wood was fabricated to imitate the crop profile in lab condition. The evaluation was comprised of two parts. First, the evaluation of edge detection algorithm in stationary state was conducted in the distorted environment comparing between manual and calculated values in terms of RMSEs in heading error and lateral deviation. Second, the evaluation of the developed tracking line algorithm was performed.

3. Results and Discussion

3.1. The evaluation of Edge detection algorithm in stationary state

A laboratory test to evaluate the LRF-based edge detection method was conducted. Fig. 8 (c) shows the view of objects installed in a laboratory where additional interfering objects were placed nearby an artificial crop profile. Considering LRF detection range and scanning angle, all of the interfering objects could be determined as noise signals except for the artificial profile and ground. Fig. 8 (a) and (b) shows the results of the 3D profile of the target objects extracted from LRF data by using the RANSAC algorithm and PTU moving in stationary. As shown as Fig. 8 (a), all of the interfering objects were filtered out and the artificial crop profile was correctly identified.
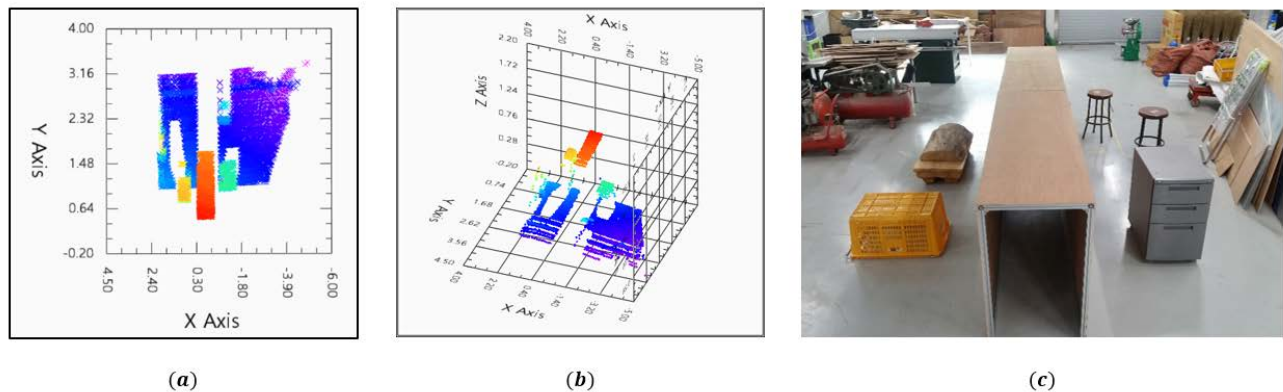

(a) (b) (c)

Fig 8. Result of 3D profile extraction using RANSAC filtering method with PTU, (a) top view (b) 3D construction (c) experimental environment

Fig. 9 shows the result of extracting edge line in distorted experimental condition shown as Fig. 8 (c). The crop edge lines were determined and updated by the maximum distance method based on the filtered LRF data processed with the RANSAC filtering every time. As shown in Fig. 9, the crop edge lines generated based on original edge points and revised edge points obtained with the proposed method are expressed as a green rhombus and a red square, respectively. Both of the crop edge lines were successfully determined when considering their geometrical definitions.

To compare the effectiveness between revision and original edge line detection methods, the lateral deviation was calculated (Table. 1). The RMS differences in position were 21.8 cm, 5.7 cm for the original tracking line and revision tracking line, respectively. Maximum lateral deviations of the original tracking line and revision tracking line were 30.4 cm and 17.8 cm and minimum lateral deviations were 17.5 cm and 2.1 cm, respectively. The results showed that the proposed method could improve the accuracy of tracking line detection performance. On the other hand, if the LRF was located on left-side and a higher place , the difference would be bigger. The RMS errors of navigation heading were 0.78 deg and 1.43 deg for the original tracking line and revision tracking line. The maximum and minimum heading errors were 2.12 deg and 0.004 deg in original edge and 4.56 deg and 0.01 deg, respectively. Although the revision edge's heading error was little bigger than the origin, that result was acceptable in real-time navigation control system.
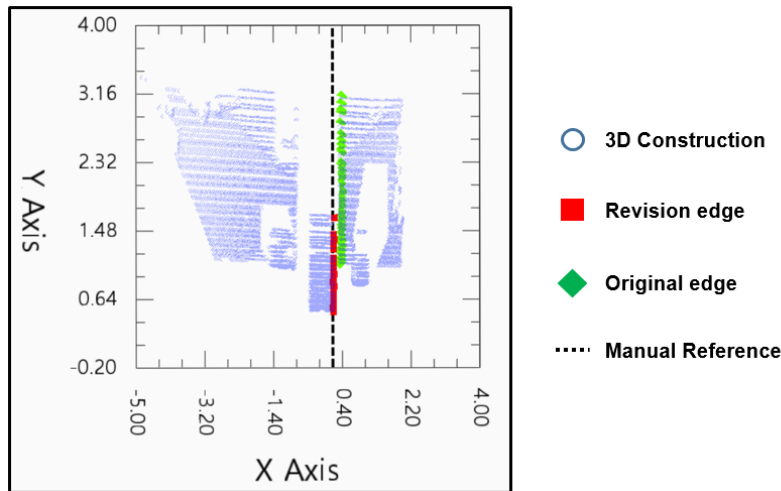
Fig 9. Result of extracting edge line in distorted environment

Table 1. The result of tracking line detection compared between original method and revision method

	Lateral RMSE(cm)	Max(cm)	Min(cm)	Heading RMSE(deg)	Max(deg)	Min(deg)
Original edge	21.81	30.48	17.54	0.78	2.12	0.004
Revision edge	5.72	10.56	2.14	1.43	4.56	0.01

3.2. The performance of navigation control in lab condition

The fundamental experiment of autonomous navigation control was conducted in a lab condition using an wooden box with a length of 2.5 m considered an artificial crop profile. The distance between reference tracking line and crop edge line, which could be maintained during autonomous navigation, was 1.5 m. The tracked vehicle was driven at 0.14 m/s. Fig. 10 shows the trajectory of the autonomous vehicle, which was calculated using rotary encoders and the kinematic model of the tracked vehicle. At first, because the distance between a starting point and the reference line was shorter than 1.5 m, the vehicle turned left. When the lateral deviation was close to 1.5 m and the heading error was bigger, the vehicle turned right smoothly and followed the path with a relatively small oscillation. The RMS difference in position was calculated to be 0.059 m when the vehicle was in steady-state. But there was a problem with an increased deviation measured when the vehicle was closer to the end, which was related to the use of points in front of the LRF of 0.1~1.7 m. Further studies include the improvement in the developed steering control algorithm for guiding the vehicle to track a curved path and detect the end points ahead.

Fig 12. The trajectory of autonomous tracked vehicle
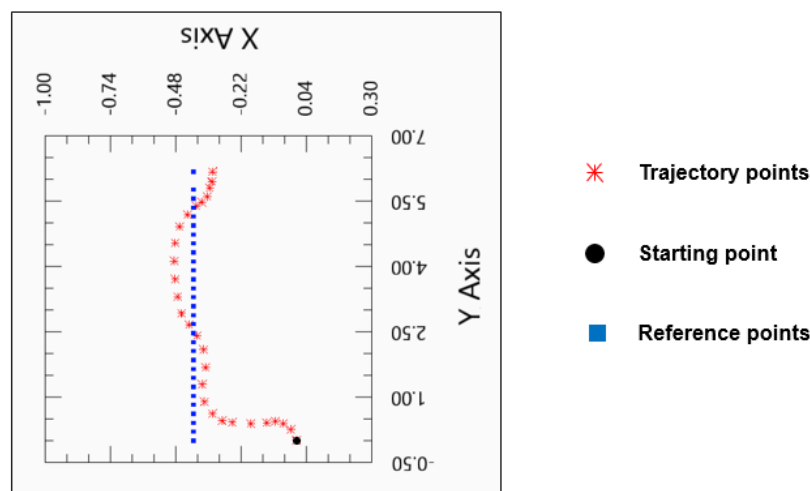
Conclusions

 A crop edge line detection algorithm was developed for an autonomous rice combine harvester using a LRF and a PTU. The results of the detection edge line in stationary state showed that the RMSEs of lateral deviation and heading error were 5.72 cm and 1.43°. This positioning and directing accuracy would be satisfactory in the design requirements with a lateral deviation < 15cm and a heading error < 5°. The fundamental navigation control algorithm developed showed its potential for real-time navigation of a crawler-type tracked vehicle. Future studies include the development of a robust landmark detection algorithm related to machine vibration and the verification of the developed tracking algorithms for field use to follow the uncut edge lines of rice crops in actual fields.

Acknowledgements

References

Ahamed, T., Takigawa, T., Koike, M. Honma, T., Hasegawa, H., & Zhang, Q. (2006). Navigation Using a Laser Range Finder for Autonomous Tractor (Part1). Journal of JSAM. 68(1), 68-77.

Barawid, O. C., Mizushima, A., Ishii, K., & Noguchi, N. (2007). Development of an autonomous navigation system using a two-dimensional laser scanner in an orchard application. Biosystems Engineering, 96(2), 139-149.

Cho, W., Iida, M., Suguri, M., Masuda, R., & Kurita, H. (2014). Using multiple sensors to detect uncut crop edges for autonomous guidance systems of head-feeding combine harvesters. Engineering in Agriculture, Environment and Food, 7(3), 115-121.

Choi, J., Yin, X., Yang, L., & Noguchi, N. (2014). Development of a laser scanner-based navigation system for a combine harvester. Engineering in Agriculture, Environment and Food, 7(1), 7-13.

Coen, T., Vanrenterghem, A., Saeys, W., & De Baerdemaeker, J. (2008). Autopilot for a combine harvester. Computers and electronics in agriculture, 63(1), 57-64.

Han, X. Z., Kim, H. J., Kim, J. Y., Yi, S. Y., Moon, H. C., Kim, J. H., & Kim, Y. J. (2015). Path-tracking simulation and field tests for an auto-guidance tillage tractor for a paddy field. Computers and Electronics in Agriculture, 112, 161-171.

Iida, M., Uchida, R., Zhu, H., Suguri, M., Kurita, H., & Masuda, R. (2013). Path-following control of a head-feeding combine robot. Engineering in Agriculture, Environment and Food, 6(2), 61-67.

Kise, M., Zhang, Q., & Más, F. R. (2005). A stereovision-based crop row detection method for tractor-automated guidance. Biosystems Engineering, 90(4), 357-367.

Teng, Z., Noguchi, N., Liangliang, Y., Ishii, K., & Jun, C. (2016). Development of uncut crop edge detection system based on laser rangefinder for combine harvesters. International Journal of Agricultural and Biological Engineering, 9(2), 21.

Torii, T., Takamizawa, A., Okamoto, T., & Imou, K. (2000). Crop row tracking by an autonomous vehicle using machine vision (Part 2). Journal-Japanese Society of Agricultural Machinery, 62(5), 37-42.